Whole Body Control of a Dual Arm Underwater Vehicle Manipulator System ⋆

E. Simetti * **G. Casalino** *

* *Interuniversity Research Center on Integrated Systems for the Marine Environment (ISME)*
Department of Computer Science, Bioengineering, Robotics, and System Engineering (DIBRIS),
University of Genova, Via Opera Pia 13, 16145 Genova, Italy
(e-mail: enrico.simetti@unige.it)

Abstract: This paper presents a whole body control framework for the control of a dual arm underwater vehicle manipulator system developed in the context of the MARIS Italian research project, which deals with the control and coordination of underwater vehicles for manipulation and transportation problems. The proposed framework is the extension of the one used in the successful TRIDENT FP7 project that has been improved to be able to deal with multidimensional inequality control objectives. After the presentation of the mathematical background, the paper presents some simulation results showing the good performances of the proposed algorithm.

Keywords: dual arm underwater manipulation, underwater vehicle manipulator system, task priority control, whole body control, hierarchical control, underwater floating manipulation

1. INTRODUCTION

Underwater vehicle manipulator systems (UVMS), also called Intervention Underwater Autonomous Vehicles (I-AUV), have been increasingly studied and exploited in the last few years. Their goal is to automatize actions currently performed by Remotely Operated Vehicles (ROVs), which have the fundamental drawback of requiring expensive support vessels equipped with dynamic positioning systems and capable of handling the tether cable, and manned submersibles, which instead require a human operator and thus can only be used for a few hours with the additional problem of placing a human being in a dangerous environment.

For these reasons, the research in this field has seen a steady increase in the past two decades. During early 90s, seminal works have been carried out at the Woods Hole Oceanographic Institute concerning the design and control compliant of underwater manipulators Yoerger et al. (1991) and the coordinated vehicle/arm control for tele-operation Schempf and Yoerger (1992). At the end of that decade, major breakthroughs were achieved in the pioneering AMADEUS project Lane et al. (1997), which covered dual-arm underwater manipulation control aspects, in the UNION project Rigaud et al. (1998) where the mechatronic assembly of an autonomous UVMS has taken place for the first time, and in the SAUVIM project Yuh et al. (1998); Marani et al. (2008) where the first successful attempts at underwater autonomous intervention were accomplished. A nice survey on the developed control architectures for underwater robots until late 90s can be found in Yuh (2000).

Another important milestone has been achieved with the TRIDENT project Sanz et al. (2012) that has demonstrated the autonomous recovery of a black-box from the sea floor Simetti et al. (2013, 2014), where for the first time a vehicle and an arm of comparable masses were controlled in a coordinated manner.

Recently, the TRITON Spanish research project Sales et al. (2014) is instead focusing on underwater intervention on a permanent observatory's panel, and has achieved some *practical* results on floating valve-turning operations Cieslak et al. (2015), although the proposed approach does not deal with the discontinuity problems that might arise with the use of the task priority framework near singularities. Furthermore, it uses the notion of "concurrent" tasks whose solution is summed to the solution of those following the task priority framework, thus violating their priorities. The panel valve-turning scenario is also the subject of the PANDORA project Lane et al. (2012), which focuses on the problem of persistent autonomy. Another on-going EU project is DexROV Gancet et al. (2015), which is dealing with the inspection and maintenance in presence of communication latencies.

The ARROWS project Allotta et al. (2015b) proposes to adapt and develop low cost autonomous underwater vehicle technologies to significantly reduce the cost of archaeological operations, covering the full extent of archaeological campaign. Within such a context, Allotta et al. (2015a) have proposed a modelling of the UVMS and a suitable grasp planning strategy and a decentralized cooperative control strategy Conti et al. (2015), which focuses on the

⋆ This work has been supported by the MIUR through the MARIS prot. 2010FBLHRJ project and by the European Commission through H2020-BG-06-2014-635491 DexROV project.

control of a team of UVMSs performing a transportation task, but does not take into account all the inequality control objectives that each UVMS needs to satisfy.

Finally, the Italian funded MARIS project Casalino et al. (2014), which is the context where the present work has been developed, focuses on the development of a unifying control framework capable of managing single, dual arm and cooperative UVMSs, tackling the problems of manipulation and transportation in underwater scenarios Manerikar et al. (2015b,a); Simetti et al. (2015).

One of the important aspects in the control of UVMS is how to effectively exploit all their degrees of freedom (DOF) for accomplishing the required tasks. This problem is further increased by analysing the actual tasks that an UVMS has to tackle. Indeed, aside from positioning the end-effector over the blackbox or the pipe to be grasped, most if not all the other tasks are dedicated to maintaining the safety of the system (avoiding the arm's joint limits, avoiding self collisions and collision with other vehicles) or certain operative configurations (i.e. keeping the object grossly centred, avoiding camera occlusions) and thus are a prerequisite for the final end-effector positioning task. These safety/operational tasks are usually accomplished whenever they are under, above or between some given thresholds, because they are inequality control objectives.

The seminal results on task/operational-based control Nakamura and Hanafusa (1986), Khatib (1987), and their successive extension with the introduction of priorities between tasks Nakamura (1991), Siciliano and Slotine (1991) did not integrate inequality control objectives efficiently. Indeed, they were converted to equality ones, overconstraining the system. This is due to the fact that, in the original formulation, activating (inserting) or deactivating (deleting) a task implies a discontinuity in the null space projector, which leads to a discontinuity in the control law Lee et al. (2012).

In the last decade, major research efforts have been spent in order to incorporate inequality control objectives in the task-based control paradigm. In Mansard et al. (2009b) a new inversion operator is introduced for the computation of a smooth inverse with the ability of enabling and disabling tasks, and has been extended to the case of a hierarchy of tasks in Mansard et al. (2009a). However, the major problem within that work is that it requires the computation of all the combinations of possible active and inactive tasks, which grows exponentially.

Another interesting approach is given in Lee et al. (2012). The idea is to modify the reference of each task that is inserted or being removed, in order to comply with the already present ones, in such a way to smooth out any discontinuity. However, the algorithm requires $m!$ pseudo inverses with m number of tasks. The authors provide also approximate solutions, which are suboptimal whenever more than one task is being activated/deactivated (in *transition*).

Previous works of the authors dealt with the control of underwater free floating manipulators Casalino et al. (2012a,b); Simetti et al. (2014) in the context of the TRIDENT project. In such works, all the tasks except the end-effector position control were represented by scalar inequality tasks. The activation and deactivation of scalar tasks was tackled in the prioritized control.

This work generalizes the framework presented in Simetti et al. (2014) and allows its use to the dual arm scenario of the MARIS project, where multidimensional inequality tasks naturally arise. It retains the simplicity of the original task-priority framework Siciliano and Slotine (1991) since it only uses pseudo-inverses. Tasks are activated and deactivated via the use of an activation matrix. The possible discontinuities that can arise with the use of an activation matrix Mansard et al. (2009a,b) are eliminated with the use of a novel task-oriented regularization and the singular value oriented one. This allows to treat inequality control objectives efficiently, as their corresponding tasks are deactivated whenever the system is inside the validity region of the inequality objective, avoiding any overconstraining of the system.

The work is structured as follows. Section 2 introduces some definitions and the main control objectives of the dual arm UVMS. Section 3 presents the underlying task priority framework that allows the UVMS to concurrently carry out its different tasks. Simulation results are presented in Section 4, and some final conclusions are given in Section 5.

2. DEFINITIONS AND PRELIMINARIES

Before starting the discussion we first introduce some notation and definitions. Then, the control objectives of the UVMS are presented and finally the basics of pseudo inverse problems are recalled.

2.1 Notation

Vectors and matrices are expressed with a bold face character, such as $\boldsymbol{M}$, whereas scalar values are represented with a normal font such as γ. Given a matrix $\boldsymbol{M}$:

- $M_{(i,j)}$ indicates the element of $\boldsymbol{M}$ at the i-th row and j-th column;
- $\boldsymbol{M}_{\{k\}}$ refers to the k-th row of $\boldsymbol{M}$;
- $\boldsymbol{M}^{\#}$ is the exact generalized pseudo-inverse (see Ben-Israel and Greville (2003) for a review on pseudo-inverses and their properties), i.e. the pseudo inverse of $\boldsymbol{M}$ performed without any regularizations.

Further, less used, notation is introduced as needed.

2.2 Definitions

Let us consider a free floating dual arm UVMS such as the one depicted in Fig. 1, and in order to avoid any confusion, let us report hereafter some definitions often used in this paper:

- the system configuration vector $\boldsymbol{c} \in \mathbb{R}^n$, which for a dual arm UVMS is

$$\boldsymbol{c} \triangleq \begin{bmatrix} \boldsymbol{q}_a \\ \boldsymbol{q}_b \\ \boldsymbol{\eta} \end{bmatrix}, \tag{1}$$

  where $\boldsymbol{q}_a \in \mathbb{R}^{l_a}$ is the arm a configuration vector, $\boldsymbol{q}_b \in \mathbb{R}^{l_b}$ is the arm b configuration vector and $\boldsymbol{\eta} \in \mathbb{R}^6$ is the vehicle *generalised coordinate position vector*,

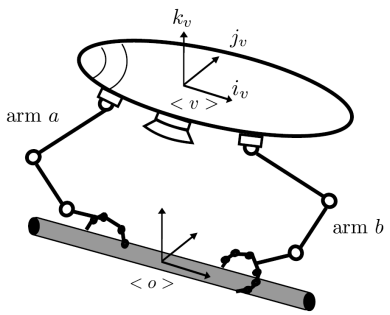

Fig. 1. Dual arm configuration with the relevant frames

which is the stacked vector of the position vector $\boldsymbol{\eta}_1$ and orientation vector $\boldsymbol{\eta}_2$, the latter expressed in terms of the three angles yaw, pitch and roll (applied in this sequence) Perez and Fossen (2007). From the above definitions it results $n = l_a + l_b + 6$;

- the system velocity vector $\dot{\boldsymbol{y}} \in \mathbb{R}^n$, which for a single vehicle manipulator system is

$$\dot{\boldsymbol{y}} \triangleq \begin{bmatrix} \dot{\boldsymbol{q}}_a \\ \dot{\boldsymbol{q}}_b \\ \boldsymbol{v} \end{bmatrix}, \tag{2}$$

where $\dot{\boldsymbol{q}}_a \in \mathbb{R}^{l_a}$ are the arm a joint velocities, $\dot{\boldsymbol{q}}_b \in \mathbb{R}^{l_b}$ are the arm b joint velocities, and $\boldsymbol{v} \in \mathbb{R}^6$ represents the vehicle's linear and angular velocities expressed on the vehicle frame $\langle v \rangle$;

- given the system configuration vector $\boldsymbol{c}$, we define an *equality control objective* an equality of the type $\boldsymbol{f}(\boldsymbol{c}) = \boldsymbol{0}$ to be eventually achieved. An example of this type of control objective is the position control of an arm's end-effector;
- we define an *inequality control objective* an inequality of the type $\boldsymbol{f}(\boldsymbol{c}) < \boldsymbol{0}$ to be eventually achieved, where the inequality is satisfied component by component. An example of this type of control objective is the avoidance of the arm's joint limits;
- we define *task* as tracking at best a suitable reference rate $\dot{\tilde{\boldsymbol{x}}}$, capable of driving the associated variable $\boldsymbol{x}$ toward the corresponding objective. For example, a task is tracking a reference velocity for the arm end-effector, which was generated in order to reach the goal position, where the corresponding control objective is satisfied;
- the control objectives may have different *priorities* and the same holds for their associated tasks. The achievement of a task with lower priority should not interfere with the achievement of a task with higher priority. Tasks with the same priority are achieved simultaneously, if possible. A set of tasks with different priorities is also called a *hierarchy of tasks*.

2.3 Control Objectives

This section presents the control objectives that the dual arm UVMS, sketched in Figure 1 has to tackle.

The simplest inequality objective that both arms must respect is that all their joints are falling within their physical limits, i.e. for each arm it must hold

$$q_{i,m} \leq q_i \leq q_{i,M} \; ; \; i = 1, \ldots, l; \tag{3}$$

with l being the number of arm joints (i.e. l_a for arm a and l_b for arm b respectively). Furthermore, each arm should avoid their singularity configurations. This can be achieved by maintaining the manipulability measure Yoshikawa (1985) above a minimum value, thus trivially leading to the following inequality type objective for each arm

$$\mu \geq \mu_m. \tag{4}$$

For the good operability of the vision algorithms, the vehicle must keep the object grossly centred into its camera field of view. This means that the modulus of the misalignment error $\boldsymbol{\xi}$, formed by the unit vector joining the origin of the object to the camera frame, and the unit vector z axis (the one perpendicular to the image plane) of the camera frame itself, must be below a certain threshold. The misalignment vector between two vectors is defined as the angle-axis around which the first vector should rotate in order to be aligned with the second one.

At the same time, the vehicle must also be closer than a given horizontal distance d_M to the vertical line passing through the object, and between a maximum and minimum height with respect to object located on the sea floor. This consequently translates into the requirement of achieving the following inequalities

$$\|\boldsymbol{\xi}\| < \xi_M \; ; \; \|\boldsymbol{d}\| \leq d_M \; ; \; h_m \leq \|\boldsymbol{h}\| \leq h_M \; ; \tag{5}$$

where $\boldsymbol{d}$ and $\boldsymbol{h}$ are the horizontal and vertical vectors.

Since the vehicle should avoid configurations with high tilt angle values, this further requires the achievement of the following additional inequality

$$\|\boldsymbol{\varphi}\| \leq \varphi_m, \tag{6}$$

where $\boldsymbol{\varphi}$ represents the misalignment vector that the absolute vertical z-axis unit vector forms with respect to the vehicle z-axis one,

Within the fulfilment of the above goals, each arm's end effector must eventually reach the object frame, for then starting the successive grasping phase. Thus the following equality objectives have to be achieved for both arms

$$\|\boldsymbol{r}\| = 0 \;\; ; \;\; \|\boldsymbol{\vartheta}\| = 0, \tag{7}$$

where $\boldsymbol{r}$ is the position error and $\boldsymbol{\vartheta}$ the orientation error.

Finally, after that the two arms have separately grasped a common object, in order to transport it to a goal location, the whole system must be suitable coordinated to also comply with the kinematic constraint that the object itself imposes, i.e.

$$\boldsymbol{J}_{t,a}\dot{\boldsymbol{q}}_a = \boldsymbol{J}_{t,b}\dot{\boldsymbol{q}}_b. \tag{8}$$

where $\boldsymbol{J}_{t,a}$ is the tool frame $\langle t \rangle$ Jacobian of the arm a once we have set $\langle t \rangle$ as coincident with $\langle o \rangle$, and where $\boldsymbol{J}_{t,b}$ is similarly defined for the arm b. Note how the vehicle velocity $\boldsymbol{v}$ does not have any influence on the minimization of the object stress, since it is naturally always complaint with the object kinematic constraint.

The presence of two arms naturally creates the need of managing efficiently multidimensional inequality tasks (e.g. the stacked manipulability task of the two arms). The next section shows the extension of the framework used in the TRIDENT project Simetti et al. (2014), which only handled scaled inequality multidimensionals, to the case of multidimensional tasks of the MARIS project.

Before doing that, the next subsection presents some preliminaries about regularized pseudo inverses.

2.4 Regularized Pseudo Inverse

Before introducing the core of this work, it is useful to recall the fundamentals of pseudo inverses and the regularization mechanism. Toward that end, let us consider the following Jacobian relationship

$$\dot{\boldsymbol{x}} = \boldsymbol{J}\dot{\boldsymbol{y}}, \tag{9}$$

with $\boldsymbol{J} \in \mathbb{R}^{m\times n}$, $\dot{\boldsymbol{y}} \in \mathbb{R}^n$ and $\dot{\boldsymbol{x}} \in \mathbb{R}^m$.

Given a reference velocity vector $\dot{\bar{\boldsymbol{x}}}$, the velocity vector $\dot{\boldsymbol{y}}$ that realizes $\dot{\bar{\boldsymbol{x}}}$ at best, in a least-squares sense, can be found as the result of the following minimization problem

$$\min_{\dot{\boldsymbol{y}}} \|\dot{\bar{\boldsymbol{x}}} - \boldsymbol{J}\dot{\boldsymbol{y}}\|^2. \tag{10}$$

The solution to the above problem can be found computing the square and taking the derivative equal to zero, which leads to

$$(\boldsymbol{J}^T\boldsymbol{J})\dot{\boldsymbol{y}} = \boldsymbol{J}^T\dot{\bar{\boldsymbol{x}}}, \tag{11}$$

which can be solved using the pseudo inverse as

$$\dot{\boldsymbol{y}} = (\boldsymbol{J}^T\boldsymbol{J})^{\#}\boldsymbol{J}^T\dot{\bar{\boldsymbol{x}}}. \tag{12}$$

The above formula refers only to the minimum norm solution. Since for the rest of the work we will focus on exploiting the residual arbitrariness in the solution, it is worth to consider the actual manifold of solutions, considering also the null space:

$$\dot{\boldsymbol{y}} = (\boldsymbol{J}^T\boldsymbol{J})^{\#}\boldsymbol{J}^T\dot{\bar{\boldsymbol{x}}} + (\boldsymbol{I} - (\boldsymbol{J}^T\boldsymbol{J})^{\#}\boldsymbol{J}^T\boldsymbol{J})\dot{\boldsymbol{z}},\ \forall\dot{\boldsymbol{z}}. \tag{13}$$

Note that, exploiting the following identities involving pseudo inverses

$$\boldsymbol{X}^{\#} = (\boldsymbol{X}^T\boldsymbol{X})^{\#}\boldsymbol{X}^T, \tag{14}$$

$$\boldsymbol{X}^{\#} = \boldsymbol{X}^T(\boldsymbol{X}\boldsymbol{X}^T)^{\#}, \tag{15}$$

then (13) can be rewritten in the following, more usual, form

$$\dot{\boldsymbol{y}} = \boldsymbol{J}^{\#}\dot{\bar{\boldsymbol{x}}} + (\boldsymbol{I} - \boldsymbol{J}^{\#}\boldsymbol{J})\dot{\boldsymbol{z}},\ \forall\dot{\boldsymbol{z}}. \tag{16}$$

Performing a regularization means changing the original minimization problem (10) by adding an additional regularization cost, as in the following

$$\min_{\dot{\boldsymbol{y}}} \|\dot{\bar{\boldsymbol{x}}} - \boldsymbol{J}\dot{\boldsymbol{y}}\|^2 + \|\dot{\boldsymbol{y}}\|^2_{\boldsymbol{R}}. \tag{17}$$

This is usually done to deal with the ill-definition of the solution near a singularity of the matrix $\boldsymbol{J}$. The solution of the regularized problem, following the same steps performed for the original one, is

$$(\boldsymbol{J}^T\boldsymbol{J} + \boldsymbol{R})\dot{\boldsymbol{y}} = \boldsymbol{J}^T\dot{\bar{\boldsymbol{x}}}, \tag{18}$$

$$\dot{\boldsymbol{y}} = (\boldsymbol{J}^T\boldsymbol{J} + \boldsymbol{R})^{\#}\boldsymbol{J}^T\dot{\bar{\boldsymbol{x}}}. \tag{19}$$

The presence of the regularizing matrix $\boldsymbol{R}$ does not allow anymore to use the identity (14) and perform the substitution as in (16). Instead, the following substitution in (16) is performed

$$\boldsymbol{J}^{\#} \rightarrow (\boldsymbol{J}^T\boldsymbol{J} + \boldsymbol{R})^{\#}\boldsymbol{J}^T \tag{20}$$

and the manifold of solutions with $\boldsymbol{J}$ regularized by $\boldsymbol{R}$ results to be

$$\dot{\boldsymbol{y}} = (\boldsymbol{J}^T\boldsymbol{J}+\boldsymbol{R})^{\#}\boldsymbol{J}^T\dot{\bar{\boldsymbol{x}}}+(\boldsymbol{I}-(\boldsymbol{J}^T\boldsymbol{J}+\boldsymbol{R})^{\#}\boldsymbol{J}^T\boldsymbol{J})\dot{\boldsymbol{z}},\ \forall\dot{\boldsymbol{z}}. \tag{21}$$

It is noteworthy to see that the projection matrix $(\boldsymbol{I} - (\boldsymbol{J}^T\boldsymbol{J}+\boldsymbol{R})^{\#}\boldsymbol{J}^T\boldsymbol{J})$ is not anymore an orthogonal projector on the null space of $\boldsymbol{J}$ whenever $\boldsymbol{R} \neq \boldsymbol{0}$.

Remark: In some works, notwithstanding the regularization of $\boldsymbol{J}$ with $\boldsymbol{R}$ in the minimum norm solution, the null space projection matrix is calculated without the regularization matrix $\boldsymbol{R}$, and thus is still an orthogonal projection. However, exploiting the non-orthogonality of the projection matrix is one of the key ideas of this work, and thus we will always consider it computed with $\boldsymbol{J}$ regularized by $\boldsymbol{R}$ as in (21). Furthermore, if the projection matrix is calculated without any regularization, a discontinuity occurs whenever an exact singularity of the matrix $\boldsymbol{J}$ is encountered.

3. WHOLE BODY CONTROL FRAMEWORK OF DUAL ARM UVMS

This section presents the whole body control framework developed for the control of dual arm UVMS. Toward that end, we first focus on the problem of dealing with multidimensional inequality control objectives and we show how classical regularization methods based on SVD are not enough to eliminate practical discontinuities that arise when trying to activate or deactivate one of such tasks. The introduction of a novel regularization, called task oriented, coupled with the SVD one, allows to create a continuously varying null space, which is exploited by a final minimization on the control vector to eliminate any practical discontinuity. Successively, the extension to the hierarchy of priority levels is presented. With this novel activation method, the task priority framework presented in Simetti et al. (2014) is straightforwardly extended to cope with the dual arm case.

3.1 Task Oriented Regularization

To begin the discussion, let us again consider the Jacobian relationship (9) and a scenario where, for some reason, one or more of these rows start losing importance, even to a point where the associated equation should not be anymore considered. In particular, for each row we consider an associated scalar value $0 \leq a \leq 1$ whose meaning is the following:

- $a = 1$ implies that the corresponding scalar task must be exactly assigned if possible, i.e. the goal is to have $\dot{x} = \dot{\bar{x}}$. We term this as an *active task*; for an inequality control objective this is the case where it is not yet satisfied, i.e. $f(\boldsymbol{c}) > 0$ and the tracking of the velocity reference is needed to reach the region where inequality is satisfied.
- $a = 0$ implies that the corresponding scalar task should not be considered, i.e. $\dot{x}$ should be unconstrained. We term this situation as a *deactivated task*; for an inequality control objective this implies that $f(\boldsymbol{c}) < -\beta < 0$, i.e. the control objective is satisfied with a given security threshold (represented by $\beta > 0$). The β value allows to create a buffer zone, where the inequality is already satisfied, but the activation value is still greater than zero. This is necessary to avoid chattering problems around the inequality control objective threshold.
- $0 < a < 1$ implies that $\dot{x}$ should smoothly evolve between the two previous cases. This is called a *task in transition*, and for an inequality control objective it means that the control objective is satisfied but not

yet to the point where it is completely safe to neglect the corresponding task, i.e. $-\beta < f(\boldsymbol{c}) < 0$.

The straightforward idea is to modify the problem (10) by adding a weight diagonal matrix $\boldsymbol{A}$, whose diagonal elements are defined as above. Following this idea, (10) becomes

$$\min_{\dot{\boldsymbol{y}}} \|\boldsymbol{A}(\dot{\tilde{\boldsymbol{x}}} - \boldsymbol{J}\dot{\boldsymbol{y}})\|^2 . \tag{22}$$

Its corresponding manifold of non-regularized solutions is

$$\dot{\boldsymbol{y}} = (\boldsymbol{AJ})^{\#}\boldsymbol{A}\dot{\tilde{\boldsymbol{x}}} + (\boldsymbol{I} - (\boldsymbol{AJ})^{\#}\boldsymbol{AJ})\dot{\boldsymbol{z}},\ \forall \dot{\boldsymbol{z}}. \tag{23}$$

Equation (23) unfortunately exhibits discontinuities in the $\dot{\boldsymbol{y}}$ when $\boldsymbol{A}$ is varied, since the weighted pseudo-inverse is invariant to the weights on the rows of $\boldsymbol{J}$ that are linearly independent Doty et al. (1993). More specifically, the discontinuity occurs whenever a value of $A_{(i,i)}$ changes from 0 to $\epsilon > 0$ and vice versa.

To deal with the problem of discontinuities, the use of the DLS (damped least squares) and SVO (singular value oriented) regularizations has been proposed. While the latter is certainly better, since it acts specifically only on the singular directions, in both cases there is not a straightforward relationship between the activation and the regularization damping values. This in turn requires either to have high damping values, which have a detrimental impact on the performances, or small ones, which do not prevent the issues with "practical" discontinuities, as highlighted in Mansard et al. (2009b).

Since simply imposing a weight $\boldsymbol{A}$ is insufficient to obtain the desired behavior of activating and deactivating some rows of $\boldsymbol{J}$ without "practical" discontinuities and that both the DLS and SVO regularization have different drawbacks, the idea is to modify the original minimization problem introducing a novel regularization, the here called *task oriented regularization*:

$$\min_{\dot{\boldsymbol{y}}} \left[\|\boldsymbol{A}(\dot{\tilde{\boldsymbol{x}}} - \boldsymbol{J}\dot{\boldsymbol{y}})\|^2 + \|\boldsymbol{J}\dot{\boldsymbol{y}}\|^2_{\boldsymbol{A}(\boldsymbol{I}-\boldsymbol{A})} \right]. \tag{24}$$

The rationale of this choice is that we want to preserve the rows that have their corresponding $A_{(i,i)} = 1$. Thus, the choice of using $\boldsymbol{A}(\boldsymbol{I} - \boldsymbol{A})$ guarantees that a regularization is added only to the rows in transition. Indeed, it is easy to see that the cost vanishes for all the rows with $A_{(i,i)} = 0$ or $A_{(i,i)} = 1$. Thus, if $\boldsymbol{A}$ is made of only such values, the regularization cost vanishes and the solution just corresponds to the pseudo inverse of the active rows (see Appendix A). The manifold of regularized solutions is now

$$\dot{\boldsymbol{y}} = (\boldsymbol{J}^T\boldsymbol{AJ})^{\#}\boldsymbol{J}^T\boldsymbol{AA}\dot{\tilde{\boldsymbol{x}}} + (\boldsymbol{I} - (\boldsymbol{J}^T\boldsymbol{AJ})^{\#}\boldsymbol{J}^T\boldsymbol{AAJ})\dot{\boldsymbol{z}},\ \forall \dot{\boldsymbol{z}}, \tag{25}$$

which can be more compactly written as

$$\begin{aligned} \dot{\boldsymbol{y}} &= (\sqrt{\boldsymbol{A}}\boldsymbol{J})^{\#}\sqrt{\boldsymbol{A}}\boldsymbol{A}\dot{\tilde{\boldsymbol{x}}} + (\boldsymbol{I} - (\sqrt{\boldsymbol{A}}\boldsymbol{J})^{\#}\sqrt{\boldsymbol{A}}\boldsymbol{AJ})\dot{\boldsymbol{z}} \\ &\triangleq \boldsymbol{\rho} + \boldsymbol{Q}\dot{\boldsymbol{z}},\ \forall \dot{\boldsymbol{z}}. \end{aligned} \tag{26}$$

However, it can be shown that (26) can still suffer of discontinuities when one of the $A_{(i,i)}$ goes to zero. The next section focuses on how to solve this problem.

3.2 Continuity of the Transition

In this section we will show how to solve the problem of the discontinuity of the control law (26). The idea is to combine the previously introduced task oriented regularization with the singular value one. The SVO regularization ensures the continuity of the pseudo inverse, making the matrix to be inverted always of constant rank m. However, as stated in Section 3.1, the problem of using only the SVO regularization is that to obtain a practical continuous transition, high values of the regularization are necessary, with a clear impact on the performances of the control. Instead, the previous sections have shown how the task oriented regularization acts as soon as the activation is lower than one, without impacting on the other rows. However, the task oriented regularization does not prevent the change of rank of the matrix to be inverted. The idea is thus to combine the task oriented regularization with the SVO one, combining the best of both regularizations:

- the task oriented regularization acts as soon as the task is being deactivated, immediately releasing its corresponding control directions, increasing the arbitrariness space of the solution;
- the singular value oriented regularization ensures the practical continuity even with small values because of the contemporaneous presence of the task oriented one.

The minimization problem (24) thus becomes

$$\min_{\dot{\boldsymbol{y}}} \left[\|\boldsymbol{A}(\dot{\tilde{\boldsymbol{x}}} - \boldsymbol{J}\dot{\boldsymbol{y}})\|^2 + \|\boldsymbol{J}\dot{\boldsymbol{y}}\|^2_{\boldsymbol{A}(\boldsymbol{I}-\boldsymbol{A})} + \left\|\boldsymbol{V}^T\dot{\boldsymbol{y}}\right\|^2_{\boldsymbol{P}} \right], \tag{27}$$

where $\boldsymbol{V}^T$ is the right orthonormal matrix of the SVD decomposition of $\boldsymbol{J}^T\boldsymbol{AJ} = \boldsymbol{U}\boldsymbol{\Sigma}\boldsymbol{V}^T$, and $\boldsymbol{P}$ is a diagonal singular value oriented regularization matrix, whose diagonal elements $p_{(i,i)}$ are a bell-shaped, finite support functions of the corresponding singular value. The manifold of solution of the above problem can be thus written as

$$\begin{aligned} \dot{\boldsymbol{y}} &= (\boldsymbol{J}^T\boldsymbol{AJ} + \boldsymbol{V}^T\boldsymbol{PV})^{\#}\boldsymbol{J}^T\boldsymbol{AA}\dot{\tilde{\boldsymbol{x}}} \\ &\quad + (\boldsymbol{I} - (\boldsymbol{J}^T\boldsymbol{AJ} + \boldsymbol{V}^T\boldsymbol{PV})^{\#}\boldsymbol{J}^T\boldsymbol{AAJ})\dot{\boldsymbol{z}} \\ &\triangleq \boldsymbol{\rho} + \boldsymbol{Q}\dot{\boldsymbol{z}},\ \forall \dot{\boldsymbol{z}}. \end{aligned} \tag{28}$$

From the above formula it is clear that the matrix $\boldsymbol{Q}$ evolves continuously with $\boldsymbol{A}$, since the $\boldsymbol{V}^T\boldsymbol{PV}$ regularization maintains the matrix to be inverted always of the same rank.

The main idea to eliminate any practical discontinuities is to exploit the arbitrariness of the solution $\dot{\boldsymbol{z}}$ in order to minimize the resulting control vector $\dot{\boldsymbol{y}}$. The rationale is simple. At the extreme values of $\boldsymbol{A}$ (i.e. only values either one or zero) the obtained solution corresponds to the pseudo inverse of only the active rows, which is the minimum norm solution obtainable while fulfilling the given tasks. Thus, the idea is to minimize the control vector as much as possible also during a task activation/deactivation transition, in order to smoothly join these two minimum-norm extrema.

The above idea can be represented by the following minimization problem:

$$\min_{\dot{\boldsymbol{z}}} \left[\|\boldsymbol{\rho} + \boldsymbol{Q}\dot{\boldsymbol{z}}\|^2 + \|(\boldsymbol{I} - \boldsymbol{Q})\dot{\boldsymbol{z}}\|^2 \right]. \tag{29}$$

The introduction of the second cost allows to penalize the use of the control directions characterized by an eigenvalue strictly less than one, due to the complementary nature of the eigenvalues of $\boldsymbol{Q}$ and $\boldsymbol{I} - \boldsymbol{Q}$. The solution of (29) is

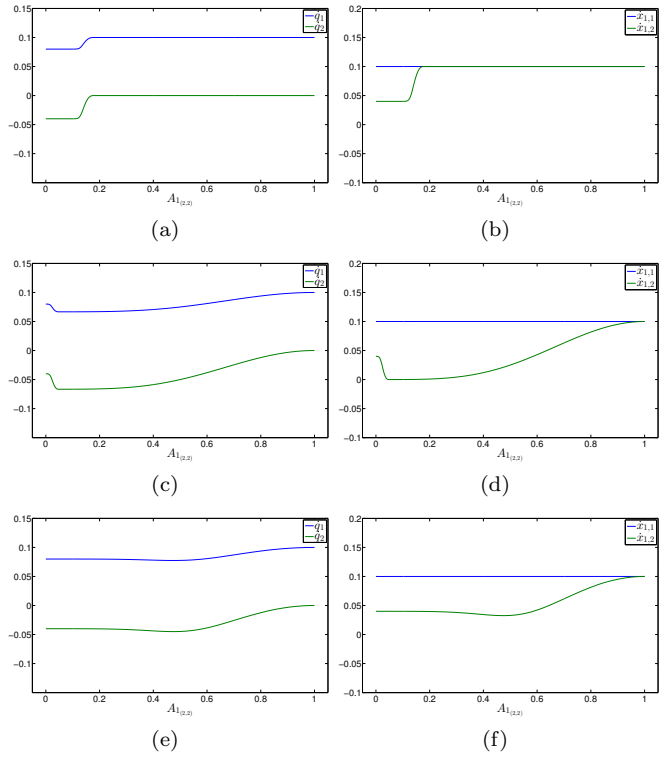

Fig. 2. Different behaviours of the control vector $\dot{\boldsymbol{y}}$ and task velocities $\dot{\boldsymbol{x}}_1$. (a), (b) represent the case with only SVO (c), (d) show the behaviour with SVO and task oriented regularization, while (e), (f) show the final behaviour when a secondary task minimizing $\dot{\boldsymbol{y}}$ is introduced.

$$\dot{\boldsymbol{z}} = -(\boldsymbol{Q}^T\boldsymbol{Q} + (\boldsymbol{I}-\boldsymbol{Q})^T(\boldsymbol{I}-\boldsymbol{Q}))^{\#}\boldsymbol{Q}^T\boldsymbol{\rho}, \tag{30}$$

which substituted into the manifold $\boldsymbol{\rho} + \boldsymbol{Q}\dot{\boldsymbol{z}}$ yields

$$\begin{aligned}\dot{\boldsymbol{y}} &= \left(\boldsymbol{I} - \boldsymbol{Q}\left(\boldsymbol{Q}^T\boldsymbol{Q} + (\boldsymbol{I}-\boldsymbol{Q})^T(\boldsymbol{I}-\boldsymbol{Q})\right)^{\#}\boldsymbol{Q}^T\right)\boldsymbol{\rho} \\ &\triangleq \boldsymbol{M}\boldsymbol{\rho}.\end{aligned} \tag{31}$$

Figure 2 shows the different behaviors depending on the choice of the applied regularizations. In the example the task Jacobian is

$$\boldsymbol{J}_1 = \begin{bmatrix} 1 & -0.5 \\ 1 & 1 \end{bmatrix}, \tag{32}$$

the velocity reference is $\dot{\tilde{\boldsymbol{x}}}_1 = [0.1\ 0.1]^T$ and the graphs show the value of the control and task velocities as the second row of $\boldsymbol{J}_1$ is activated/deactivated. The first two sub-figures show that the use of SVO alone is insufficient to provide a "practical" continuous transition over the whole interval, as already stated. The successive two sub-figures show that the addition of the task oriented regularization modifies the behavior as soon as the value of the activation becomes different than one. The final two sub-figures show that the addition of the $\dot{\boldsymbol{y}}$ minimization, combined with the SVO and the task oriented regularization provides a "practical" continuous transition over the whole interval.

3.3 Extension to Task Priority Framework

In this section, we shall first tackle the possible discontinuities that can arise when a second level of priority is introduced, and then generalize the proposed framework to any number of priority levels.

Smoothing the Discontinuities in the Prioritized Control Let us now consider another task that has to be executed with lower priority, represented by the following Jacobian relationship

$$\dot{\boldsymbol{x}}_2 = \boldsymbol{J}_2\dot{\boldsymbol{y}}, \tag{33}$$

with $\boldsymbol{J}_2 \in \mathbb{R}^{m_2\times n}$, $\dot{\boldsymbol{y}} \in \mathbb{R}^n$ and $\dot{\boldsymbol{x}}_2 \in \mathbb{R}^{m_2}$. The minimization for this second task must be performed taking into account that $\dot{\boldsymbol{y}}$ has been partially fixed by the higher priority task. The manifold of solutions of the first task is given by (28) and is $\dot{\boldsymbol{y}} = \boldsymbol{\rho}_1 + \boldsymbol{Q}_1\dot{\boldsymbol{z}}_1$. Let us remark how, for the time being, we are not considering the minimization on the control vector, because that completely consumes any residual arbitrariness. We shall later see in Section 3.3.2 how that minimization is used in a hierarchy of tasks.

With that in mind, the second minimization problem can only exploit the arbitrariness of $\dot{\boldsymbol{z}}_1$, leading to

$$\begin{aligned}\min_{\dot{\boldsymbol{z}}_1} \Big[&\left\|\boldsymbol{A}_2(\dot{\tilde{\boldsymbol{x}}}_2 - \boldsymbol{J}_2\boldsymbol{Q}_1\dot{\boldsymbol{z}}_1)\right\|^2 + \|\boldsymbol{J}_2\boldsymbol{Q}_1\dot{\boldsymbol{z}}_1\|^2_{\boldsymbol{A}_2(\boldsymbol{I}-\boldsymbol{A}_2)} \\ &+ \left\|\boldsymbol{V}_2^T\dot{\boldsymbol{z}}_1\right\|^2_{\boldsymbol{P}_2}\Big],\end{aligned} \tag{34}$$

with the definition $\dot{\tilde{\boldsymbol{x}}}_2 \triangleq \dot{\tilde{\boldsymbol{x}}}_2 - \boldsymbol{J}_2\boldsymbol{\rho}_1$, and where the same task oriented and SVO regularizations have been employed to deal with the activation matrix $\boldsymbol{A}_2$.

Whenever a second level of priority is considered, a new source of possible discontinuities is represented by the non-orthogonal projection matrix $\boldsymbol{Q}_1$. To focus only on the discontinuities created by the projection matrix and to simplify the notation, let us suppose, without loss of generality, $\boldsymbol{A}_2 = \boldsymbol{I}$ and for the moment let us neglect the presence of the SVO regularization. Then, the solution of the previous minimization is

$$\dot{\boldsymbol{z}}_1 = (\boldsymbol{J}_2\boldsymbol{Q}_1)^{\#}\dot{\tilde{\boldsymbol{x}}}_2 \tag{35}$$

which substituted into the first control law leads to

$$\boldsymbol{\rho}_2 = \boldsymbol{\rho}_1 + \boldsymbol{Q}_1(\boldsymbol{J}_2\boldsymbol{Q}_1)^{\#}\dot{\tilde{\boldsymbol{x}}}_2. \tag{36}$$

Note that $\boldsymbol{Q}_1(\boldsymbol{J}_2\boldsymbol{Q}_1)^{\#}$ is in actuality the weighted pseudo-inverse, with weights $\boldsymbol{Q}_1^{-1}$ on the control vector $\dot{\boldsymbol{y}}$ Nakamura (1991).

However, the above solution, while weighting the control directions, thus preferring to use those that have an eigenvalue of $\lambda_i = 1$ (i.e. unconstrained), fails under certain conditions. Indeed, there are cases where control directions with an eigenvalue $0 < \lambda_i < 1$ are treated as if $\lambda_i = 1$, because of possible invariance of the minimization with respect to the weights Doty et al. (1993). This means that, even if the corresponding control direction only begins to be released by the higher priority tasks, the current priority level would consider it as totally free, leading to discontinuities.

To solve this problem, the idea is to compute a new task reference in lieu of $\dot{\tilde{\boldsymbol{x}}}_2$. In particular, we want to find which is the best velocity obtainable minimizing the use of control directions in transition. Toward that end, we exploit the following auxiliary problem

$$\begin{aligned}\min_{\dot{\boldsymbol{u}}_1} \Big[&\left\|\boldsymbol{A}_2(\dot{\tilde{\boldsymbol{x}}}_2 - \boldsymbol{J}_2\boldsymbol{Q}_1\dot{\boldsymbol{u}}_1)\right\|^2 + \|\boldsymbol{J}_2\boldsymbol{Q}_1\dot{\boldsymbol{u}}_1\|^2_{\boldsymbol{A}_2(\boldsymbol{I}-\boldsymbol{A}_2)} \\ &+ \|(\boldsymbol{I}-\boldsymbol{Q}_1)\dot{\boldsymbol{u}}_1\|^2 + \left\|\hat{\boldsymbol{V}}_2^T\dot{\boldsymbol{u}}_1\right\|^2_{\hat{\boldsymbol{P}}_2}\Big],\end{aligned} \tag{37}$$

where this time $\hat{\boldsymbol{V}}_2^T$ is the right orthonormal matrix of the SVD decomposition of $\boldsymbol{Q}_1^T\boldsymbol{J}_2^T\boldsymbol{A}_2\boldsymbol{J}_2\boldsymbol{Q}_1+(\boldsymbol{I}-\boldsymbol{Q}_1)^T(\boldsymbol{I}-\boldsymbol{Q}_1)$. The corresponding task velocity is

$$\dot{\boldsymbol{x}}_2^* = \boldsymbol{J}_2\boldsymbol{Q}_1\dot{\boldsymbol{u}}_1 \triangleq \boldsymbol{W}_2\dot{\tilde{\boldsymbol{x}}}_2, \tag{38}$$

which is then used as a reference velocity in (34). We then have the following results:

- if $\dot{\boldsymbol{u}}_1$ is such that $\dot{\boldsymbol{x}}_2^* = \dot{\tilde{\boldsymbol{x}}}_2$, then $\dot{\boldsymbol{z}}_1$ will be the minimum norm solution that gives $\dot{\tilde{\boldsymbol{x}}}_2$, just as in (35). Furthermore, in this case $\boldsymbol{W}_2 = \boldsymbol{I}$;
- conversely, $\dot{\boldsymbol{z}}_1 = \dot{\boldsymbol{u}}_1$ and the obtained $\dot{\boldsymbol{x}}_2$ will necessarily differ from $\dot{\tilde{\boldsymbol{x}}}_2$ because not enough unconstrained control directions are available to obtain the desired velocity.

In practice, $\boldsymbol{Q}_1(\boldsymbol{J}_2\boldsymbol{Q}_1)^{\#}\boldsymbol{W}_2\dot{\tilde{\boldsymbol{x}}}_2$ operates in this way: first it finds the best $\dot{\boldsymbol{x}}_2^* = \boldsymbol{W}_2\dot{\tilde{\boldsymbol{x}}}_2$ that can be obtained minimizing the use of control directions in transition, and then it exploits the standard weighted pseudo-inverse to obtain the corresponding weighted minimum norm solution (i.e. $\boldsymbol{Q}_1(\boldsymbol{J}_2\boldsymbol{Q}_1)^{\#}\dot{\boldsymbol{x}}_2^*$).

Minimization of the Control Vector as the Final Task In the previous section we have seen how to deal with a secondary task, exploiting (37) to cope with fact that the standard weighted pseudo inverse $\boldsymbol{Q}_1(\boldsymbol{J}_2\boldsymbol{Q}_1)^{\#}$ is insufficient.

Let us now go back to the minimization of the control vector presented in Section 3.2. It is clear that such a minimization can actually be seen as another task to be executed. This can be simply done considering $\boldsymbol{J}_2 = \boldsymbol{I}$, $\boldsymbol{A}_2 = \boldsymbol{I}$ and $\dot{\tilde{\boldsymbol{x}}}_2 = 0$. Then, we can see how (29) is just a special instance of (37).

This task should be placed as the very last task of the hierarchy, consuming all the residual arbitrariness to ensure continuous transitions without any practical discontinuity.

Unifying Formula for the Pseudo Inverse Before proceeding to the extension to any number of priority levels, let us first introduce a more compact notation by introducing the operator $(\cdot)^{\#,\boldsymbol{A},\boldsymbol{Q}}$ as in the following:

$$\begin{aligned}\boldsymbol{X}^{\#,\boldsymbol{A},\boldsymbol{Q}} \triangleq \big(&\boldsymbol{X}^T\boldsymbol{A}\boldsymbol{X} + (\boldsymbol{I}-\boldsymbol{Q})^T(\boldsymbol{I}-\boldsymbol{Q}) + \\ &+\boldsymbol{V}^T\boldsymbol{P}\boldsymbol{V}\big)^{\#}\boldsymbol{X}^T\boldsymbol{A}\boldsymbol{A}\end{aligned} \tag{39}$$

where $\boldsymbol{V}$ is the right orthonormal matrix of the SVD decomposition of $\boldsymbol{X}^T\boldsymbol{A}\boldsymbol{X} + (\boldsymbol{I}-\boldsymbol{Q})^T(\boldsymbol{I}-\boldsymbol{Q})$ and $\boldsymbol{P}$ is the same defined in (27).

The task oriented regularization (27) can be simply obtained by writing $\boldsymbol{J}^{\#,\boldsymbol{A},\boldsymbol{I}}$ or $\boldsymbol{J}^{\#,\boldsymbol{A},\cdot}$ to highlight the fact that the third cost vanishes from the minimization problem. Finally, the auxiliary problem (37) can be obtained by writing $(\boldsymbol{J}\boldsymbol{Q})^{\#,\boldsymbol{A},\boldsymbol{Q}}$.

3.4 Extension to Any Number of Priority Levels

Putting all the pieces together, and with the definition of the pseudo inverse given in the previous section, the extension to any number of priority levels is straightforward. With the initializations

$$\boldsymbol{\rho}_0 = \boldsymbol{0}, \quad \boldsymbol{Q}_0 = \boldsymbol{I}, \tag{40}$$

then for $k = 1, \ldots, N$, where N is the total number of the tasks:

$$\begin{aligned}\boldsymbol{W}_k &= \boldsymbol{J}_k\boldsymbol{Q}_{k-1}(\boldsymbol{J}_k\boldsymbol{Q}_{k-1})^{\#,\boldsymbol{A}_k,\boldsymbol{Q}_{k-1}} \\ \boldsymbol{Q}_k &= \boldsymbol{Q}_{k-1}(\boldsymbol{I} - (\boldsymbol{J}_k\boldsymbol{Q}_{k-1})^{\#,\boldsymbol{A}_k,\cdot}\boldsymbol{J}_k\boldsymbol{Q}_{k-1}) \\ \boldsymbol{T}_k &\triangleq (\boldsymbol{I} - \boldsymbol{Q}_{k-1}(\boldsymbol{J}_k\boldsymbol{Q}_{k-1})^{\#,\boldsymbol{A}_k,\cdot}\boldsymbol{W}_k\boldsymbol{J}_k) \\ \boldsymbol{\rho}_k &= \boldsymbol{T}_k\boldsymbol{\rho}_{k-1} + \boldsymbol{Q}_{k-1}(\boldsymbol{J}_k\boldsymbol{Q}_{k-1})^{\#,\boldsymbol{A}_k,\cdot}\boldsymbol{W}_k\dot{\tilde{\boldsymbol{x}}}_k\end{aligned} \tag{41}$$

thus ending up with the final control law

$$\dot{\boldsymbol{y}} = \boldsymbol{\rho}_N \tag{42}$$

because, according to Section 3.3.2, the N-th and final task should be the minimization of the control vector $\dot{\boldsymbol{y}}$, which consumes any residual arbitrariness.

4. SIMULATION RESULTS

In this section we present a simulation using the proposed task-priority framework for whole body dual arm UVMS control, where a fully-actuated vehicle endowed with two 7 DOFs arms is accomplishing a transportation task. In considered simulated environment, the UVMS starts from a position (in meters) of [0 0 0] with the object firmly grasped by its two arms. A common tool frame $\langle t\rangle$ is placed at the center of the object, in correspondence of the object frame $\langle o\rangle$, at about 30 cm distance from the two arms' end-effectors, and its initial position results to be in [−0.4078 0 0.9125] due to the initial postures of the arms. The goal of the transportation task is to bring the object frame $\langle o\rangle$ in the position [3 1 4] with a rotation described by a roll angle of $\pi/5$, a pitch angle of $\pi/5$ and a yaw angle of $\pi/2$.

The tasks that the UVMS has to execute are, in order of priority

(1) minimizing the interaction on the object, i.e. the velocities of the two arms end-effectors once transferred to the common object frame should be equal (a 6 dimensional equality task);
(2) avoid both arms joint limits (a 14 dimensional inequality task, one for each joint);
(3) maintain both arms with a good dexterity to avoid singular postures (a 2 dimensional inequality task);
(4) keep the vehicle with a horizontal attitude (a scalar inequality task);
(5) moving the two end-effectors in the required final goal position (a 12 dimension equality task).

Figure 3 reports the control vector generated during this simulation, showing how the arms (Fig. 3(a) and Fig. 3(b)) and the vehicle requested velocities are continuous (see Fig. 3(c) for the vehicle linear velocities and Fig. 3(d) for the angular ones). The successive Fig. 4(a) reports the time history of the arm a joint limits activation functions, while the arm b ones have not been reported since they were zero during all the trial. Figure 4(b) reports the time history of the other tasks activation functions, showing in particular how the manipulability task has been in transition for both arm a and arm b without causing problems to the generated system velocities. The successive Fig. 4(c) shows the convergence of the object position to the desired one. Finally, Fig. 5 shows some snapshots of the UVMS performing the required transportation task.

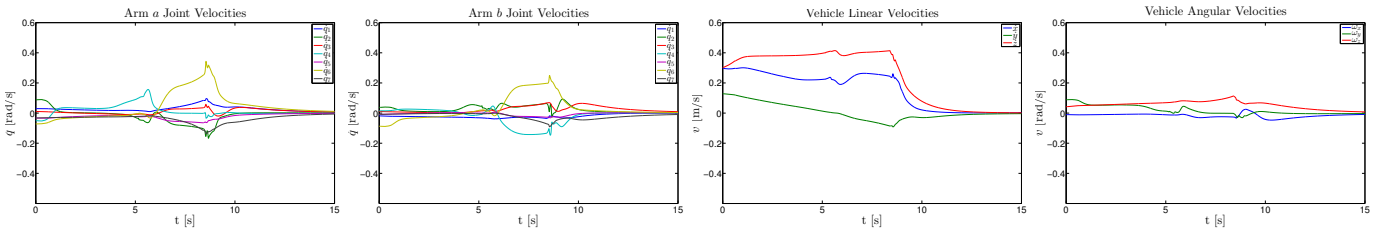

(a) (b) (c) (d)

Fig. 3. Dual arm simulation: (a) arm a joint velocities, (b) arm b joint velocities (c) vehicle linear velocity (d) vehicle angular velocity.

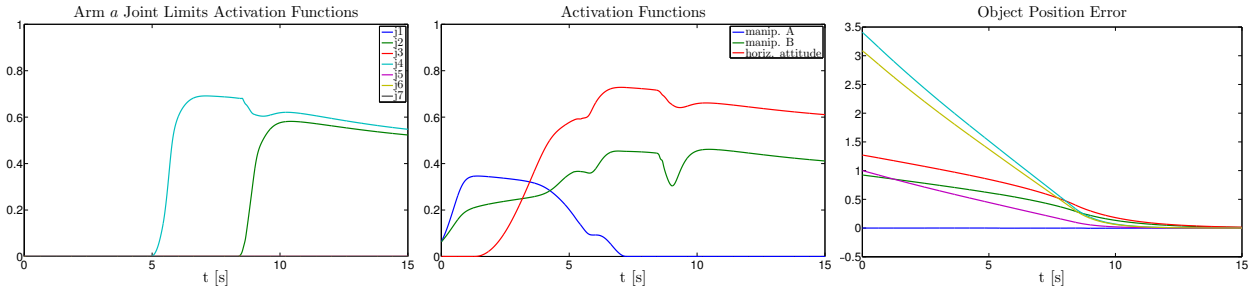

(a) (b) (c)

Fig. 4. Dual arm simulation: (a) activation functions for the joint limits task for arm a, (b) activation functions for the other tasks (c) object position error.

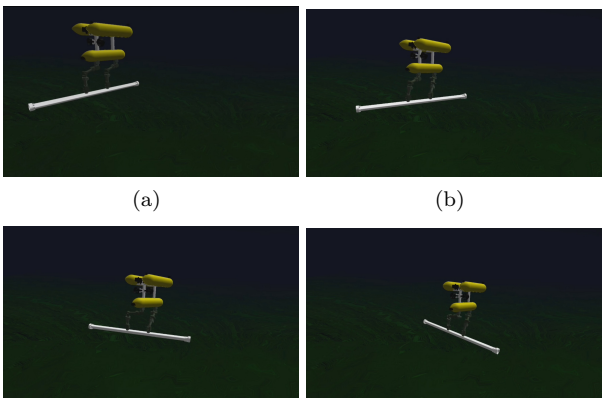

(a) (b) (c) (d)

Fig. 5. Snapshots of the UVMS performing the required transportation task.

5. CONCLUSIONS AND FUTURE WORKS

The paper has presented a task-priority based control of dual arm underwater floating manipulators. Starting from the results of the TRIDENT project Simetti et al. (2014), we have extended the core framework to encompass the activation and deactivation of multidimensional tasks. This in turns allows the introduction of multidimensional inequality control objectives, since each row can now be activated/deactivated independently from the others without incurring in "practical" discontinuities, as the simulation results have shown.

The MARIS project is now focusing on the experimental trials of a single underwater manipulator system. Other relevant activities carried out within the project regard the improvement of the vision based techniques for object pose estimation Rizzini et al. (2015), adaptive dynamic control Antonelli and Cataldi (2014), visible light communications Cossu et al. (2013) and studies on UVMS single range observability Parlangeli and Indiveri (2014). Future works will be focused on the implementation and experimentation of the cooperative control strategies presented in Manerikar et al. (2015b,a); Simetti et al. (2015) and may include the addition of velocity saturations in the prioritized control, in a similar manner as developed in Antonelli et al. (2009).

REFERENCES

Allotta, B., Conti, R., Costanzi, R., Fanelli, F., Meli, E., and Ridolfi, A. (2015a). Towards next generation intervention autonomous underwater vehicles (i-auv): development of innovative mobile manipulation techniques. In *VI International Conference on Computational Methods in Marine Engineering MARINE*. Rome, Italy.

Allotta, B., Costanzi, R., Ridolfi, A., Colombo, C., Bellavia, F., Fanfani, M., Pazzaglia, F., Salvetti, O., Moroni, D., Pascali, M.A., et al. (2015b). The arrows project: adapting and developing robotics technologies for underwater archaeology. In *IFAC workshop on navigation and control of underwater vehicles (NGCUV 2015). Girona, Spain.*

Antonelli, G. and Cataldi, E. (2014). Recursive adaptive control for an underwater vehicle carrying a manipulator. In *Control and Automation (MED), 2014 22nd Mediterranean Conference of*, 847–852. IEEE.

Antonelli, G., Indiveri, G., and Chiaverini, S. (2009). Prioritized closed-loop inverse kinematic algorithms for redundant robotic systems with velocity saturations. In *Intelligent Robots and Systems, 2009. IROS 2009. IEEE/RSJ International Conference on*, 5892–5897. IEEE.

Ben-Israel, A. and Greville, T. (2003). *Generalized inverses: theory and applications*, volume 15. Springer Verlag.

Casalino, G., Zereik, E., Simetti, E., Torelli, S., Sperindé, A., and Turetta, A. (2012a). Agility for underwater floating manipulation task and subsystem priority based control strategy. In *International Conference on Intelligent Robots and Systems (IROS 2012)*, 1772–1779. Vilamoura, Portugal. doi:10.1109/IROS.2012.6386127.

Casalino, G., Zereik, E., Simetti, E., Torelli, S., Sperindé, A., and Turetta, A. (2012b). A task and subsystem priority based control strategy for underwater floating manipulators. In *IFAC Workshop on Navigation, Guidance and Control of Underwater Vehicles (NGCUV 2012)*, 170–177. Porto, Portugal. doi:10.3182/20120410-3-PT-4028.00029.

Casalino, G., Caccia, M., Caiti, A., Antonelli, G., Indiveri, G., Melchiorri, C., and Caselli, S. (2014). Maris: A national project on marine robotics for interventions. In *Control and Automation (MED), 2014 22nd Mediterranean Conference of*, 864–869. IEEE.

Cieslak, P., Ridao, P., and Giergiel, M. (2015). Autonomous underwater panel operation by girona500 uvms: A practical approach to autonomous underwater manipulation. In *Robotics and Automation (ICRA), 2015 IEEE International Conference on*, 529–536. IEEE.

Conti, R., Meli, E., Ridolfi, A., and Allotta, B. (2015). An innovative decentralized strategy for i-auvs cooperative manipulation tasks. *Robotics and Autonomous Systems*, 72, 261–276.

Cossu, G., Corsini, R., Khalid, A., Balestrino, S., Coppelli, A., Caiti, A., and Ciaramella, E. (2013). Experimental demonstration of high speed underwater visible light communications. In *Optical Wireless Communications (IWOW), 2013 2nd International Workshop on*, 11–15. IEEE.

Doty, K.L., Melchiorri, C., and Bonivento, C. (1993). Theory of generalized inverses applied to robotics. *International Journal of Robotics Research*, 12(1), 1–19.

Gancet, J., Urbina, D., Letier, P., Ilzokvitz, M., Weiss, P., Gauch, F., Antonelli, G., Indiveri, G., Casalino, G., Birk, A., et al. (2015). Dexrov: Dexterous undersea inspection and maintenance in presence of communication latencies. In *IFAC Workshop on Navigation, Guidance and Control of Underwater Vehicles (NGCUV)*.

Khatib, O. (1987). A unified approach for motion and force control of robot manipulators: The operational space formulation. *Robotics and Automation, IEEE Journal of*, 3(1), 43–53.

Lane, D.M., Davies, J.B.C., Casalino, G., Bartolini, G., Cannata, G., Veruggio, G., Canals, M., Smith, C., O'Brien, D.J., Pickett, M., Robinson, G., Jones, D., Scott, E., Ferrara, A., Angelleti, D., Coccoli, M., Bono, R., Virgili, P., Pallas, R., and Gracia, E. (1997). Amadeus: advanced manipulation for deep underwater sampling. *IEEE Robot Autom Mag*, 4(4), 34–45.

Lane, D.M., Maurelli, F., Kormushev, P., Carreras, M., Fox, M., and Kyriakopoulos, K. (2012). Persistent autonomy: the challenges of the pandora project. In *Proceedings of IFAC MCMC*.

Lee, J., Mansard, N., and Park, J. (2012). Intermediate desired value approach for task transition of robots in kinematic control. *IEEE Transactions on Robotics*, 28(6), 1260–1277.

Manerikar, N., Casalino, G., Simetti, E., Torelli, S., and Sperindé, A. (2015a). On autonomous cooperative underwater floating manipulation systems. In *International Conference on Robotics and Automation (ICRA 15)*, 523–528. Seattle, WA.

Manerikar, N., Casalino, G., Simetti, E., Torelli, S., and Sperindé, A. (2015b). On cooperation between autonomous underwater floating manipulation systems. In *Underwater Technology 2015*, 1–6. Chennai, India. doi:10.1109/UT.2015.7108310.

Mansard, N., Khatib, O., and Kheddar, A. (2009a). A unified approach to integrate unilateral constraints in the stack of tasks. *IEEE Trans. Robot.*, 25(3), 670–685.

Mansard, N., Remazeilles, A., and Chaumette, F. (2009b). Continuity of varying-feature-set control laws. *IEEE Trans. on Automatic Control*, 54(11), 2493–2505.

Marani, G., Choi, S.K., and Yuh, J. (2008). Underwater autonomous manipulation for intervention missions AUVs. *Ocean Engineering*, 36, 15–23.

Nakamura, Y. (1991). *Advanced Robotics: Redundancy and Optimization*. Addison Wesley.

Nakamura, Y. and Hanafusa, H. (1986). Inverse kinematic solutions with singularity robustness for robot manipulator control. *Journal of Dynamic Systems, Measurement and Control*, 108, 163–171.

Parlangeli, G. and Indiveri, G. (2014). Single range observability for cooperative underactuated underwater vehicles. In *Proceedings of the 19th IFAC World Congress*, volume 19, 5127–5138.

Perez, T. and Fossen, T.I. (2007). Kinematic models for manoeuvring and seakeeping of marine vessels. *Modeling, Identification and Control*, 28(1), 19–30.

Rigaud, V., Coste-Manière, È., Aldon, M.J., Probert, P., Perrier, M., Rives, P., Simon, D., Lang, D., Kiener, J., Casal, A., et al. (1998). Union: underwater intelligent operation and navigation. *Robotics & Automation Magazine, IEEE*, 5(1), 25–35.

Rizzini, D.L., Kallasi, F., Oleari, F., and Caselli, S. (2015). Investigation of vision-based underwater object detection with multiple datasets. *Int J Adv Robot Syst*, 12(77), 1–13.

Sales, J., Santos, L., Sanz, P.J., Dias, J., and García, J.C. (2014). Increasing the autonomy levels for underwater intervention missions by using learning and probabilistic techniques. In *ROBOT2013: First Iberian Robotics Conference*, 17–32. Springer.

Sanz, P., Ridao, R., Oliver, G., Casalino, P., Insaurralde, C., Silvestre, C., Melchiorri, M., and Turetta, A. (2012). Trident: Recent improvements about autonomous underwater intervention missions. In *Proceedings of the IFAC Workshop on Navigation, Guidance and Control of Underwater Vehicles (NGCUV2012), Porto, Portugal*.

Schempf, H. and Yoerger, D. (1992). Coordinated vehicle/manipulator design and control issues for underwater telemanipulation. In *IFAC Control Applications in Marine Systems (CAMS 92)*. Genova, Italy.

Siciliano, B. and Slotine, J.J.E. (1991). A general framework for managing multiple tasks in highly redundant robotic systems. In *Proc. Fifth Int Advanced Robotics 'Robots in Unstructured Environments', 91 ICAR. Conf*,

1211–1216. Pisa, Italy.

Simetti, E., Casalino, G., Manerikar, N., Torelli, S., Sperindé, A., and Wanderlingh, F. (2015). Cooperation between autonomous underwater vehicle manipulations systems with minimal information exchange. In *IEEE/MTS OCEANS 2015*. Genova, Italy.

Simetti, E., Casalino, G., Torelli, S., Sperindé, A., and Turetta, A. (2013). Experimental results on task priority and dynamic programming based approach to underwater floating manipulation. In *OCEANS 2013*. Bergen, Norway. doi:10.1109/OCEANS-Bergen.2013.6608016.

Simetti, E., Casalino, G., Torelli, S., Sperindé, A., and Turetta, A. (2014). Floating underwater manipulation: Developed control methodology and experimental validation within the trident project. *Journal of Field Robotics*, 31(3), 364–385. doi:10.1002/rob.21497.

Yoerger, D.R., Schempf, H., and DiPietro, D.M. (1991). Design and performance evaluation of an actively compliant underwater manipulator for full-ocean depth. *Journal of robotic systems*, 8(3), 371–392.

Yoshikawa, T. (1985). Manipulability of robotic mechanisms. *Int. J. of Robotics Research*, 4(1), 3–9.

Yuh, J., Choi, S., Ikehara, C., Kim, G., McMurty, G., Ghasemi-Nejhad, M., Sarkar, N., and Sugihara, K. (1998). Design of a semi-autonomous underwater vehicle for intervention missions (SAUVIM). In *Underwater Technology, 1998. Proceedings of the 1998 International Symposium on*, 63–68. IEEE, Tokyo, Japan.

Yuh, J. (2000). Design and control of autonomous underwater robots: A survey. *Autonomous Robots*, 8(1), 7–24.

Appendix A. RESIDUAL ORTHOGONALITY PROPERTIES OF THE PROJECTOR

In the classical task priority framework the projection operator is orthogonal, and guarantees that lower priority task can only act inside the null space of the higher priority ones. This ensures the invariance of the main task w.r.t. lower priority ones. However, in our proposed solution, the projection matrix (see the definition of $\boldsymbol{Q}$ in (26)) is not orthogonal whenever any of the activation values are different from 0 and 1, i.e. whenever any task is in the transition zone. In this section we analyse the residual orthogonality properties of the proposed projector.

Toward that end let us recall the minimization problem with the task oriented regularization (24)

$$\min_{\dot{\boldsymbol{y}}} \left[\|\boldsymbol{A}(\dot{\bar{\boldsymbol{x}}} - \boldsymbol{J}\dot{\boldsymbol{y}})\|^2 + \|\boldsymbol{J}\dot{\boldsymbol{y}}\|^2_{\boldsymbol{A}(\boldsymbol{I}-\boldsymbol{A})} \right],$$

whose manifold of regularized solutions (26) is recalled hereafter

$$\begin{aligned}\dot{\boldsymbol{y}} &= (\sqrt{\boldsymbol{A}}\boldsymbol{J})^{\#}\sqrt{\boldsymbol{A}}\boldsymbol{A}\dot{\bar{\boldsymbol{x}}} + (\boldsymbol{I} - (\sqrt{\boldsymbol{A}}\boldsymbol{J})^{\#}\sqrt{\boldsymbol{A}}\boldsymbol{A}\boldsymbol{J})\dot{\boldsymbol{z}} \\ &\triangleq \boldsymbol{\rho} + \boldsymbol{Q}\dot{\boldsymbol{z}},\ \forall \dot{\boldsymbol{z}}.\end{aligned}$$

Let us prove the fact that, under some assumptions, the projection matrix admits some residual orthogonality property: it is orthogonal with respect to the active rows of $\boldsymbol{J}$, i.e. $(\boldsymbol{J}\boldsymbol{Q})_{\{i\}} = \boldsymbol{0}$ for every i-th row for which $A_{(i,i)} = 1$. Toward that end, let us start the discussion by considering $A_{(i,i)} > 0, \forall i$ and $\boldsymbol{J}$ full rank, which implies that $\sqrt{\boldsymbol{A}}\boldsymbol{J}$ is full row rank. After some simple algebra we get

$$\dot{\boldsymbol{y}} = \boldsymbol{J}^{\#}\boldsymbol{A}\dot{\bar{\boldsymbol{x}}} + (\boldsymbol{I} - \boldsymbol{J}^{\#}\boldsymbol{A}\boldsymbol{J})\dot{\boldsymbol{z}} \triangleq \boldsymbol{\rho} + \boldsymbol{Q}\dot{\boldsymbol{z}},\ \forall \dot{\boldsymbol{z}}. \tag{A.1}$$

It is easy to see that the projection matrix $(\boldsymbol{I} - \boldsymbol{J}^{\#}\boldsymbol{A}\boldsymbol{J})$ is actually orthogonal to the active rows. Indeed, multiplying the projector by $\boldsymbol{J}$ yields

$$\boldsymbol{J}(\boldsymbol{I} - \boldsymbol{J}^{\#}\boldsymbol{A}\boldsymbol{J}) = (\boldsymbol{J} - \boldsymbol{J}\boldsymbol{J}^{\#}\boldsymbol{A}\boldsymbol{J}) = (\boldsymbol{I} - \boldsymbol{A})\boldsymbol{J} \tag{A.2}$$

since $\boldsymbol{J}\boldsymbol{J}^{\#} = \boldsymbol{I}$ under the above assumptions. The above result implies that, for every row where $A_{(i,i)} = 1$, then $(\boldsymbol{J}\boldsymbol{Q})_{\{i\}} = \boldsymbol{0}$ as it was claimed. However, the projection matrix $\boldsymbol{Q}$ does not prevent $\dot{\boldsymbol{z}}$ from influencing the other rows. As said before, this is a positive fact, as those rows are being deactivated and thus there is not anymore any need to guarantee the fulfilment of their corresponding velocity reference. Indeed, when $A_{(i,i)}$ reaches zero, the corresponding velocity should be unconstrained.

Let us now drop the two assumptions of full rankness of $\boldsymbol{A}$ and $\boldsymbol{J}$. Without losing generality, let us suppose that the rows with $A_{(i,i)} = 0$ are at the bottom, and let us partition $\boldsymbol{A}$ and $\boldsymbol{J}$ in the following way

$$\boldsymbol{A} = \begin{bmatrix} \bar{\boldsymbol{A}} & \boldsymbol{0} \\ \boldsymbol{0} & \boldsymbol{0} \end{bmatrix} \ ; \ \boldsymbol{J} = \begin{bmatrix} \bar{\boldsymbol{J}} \\ \hat{\boldsymbol{J}} \end{bmatrix}, \tag{A.3}$$

where $\bar{\boldsymbol{J}}$ only contains the i-th rows for which $A_{(i,i)} \neq \boldsymbol{0}$. Given the above definition we have that

$$\sqrt{\boldsymbol{A}}\boldsymbol{J} = \begin{bmatrix} \sqrt{\bar{\boldsymbol{A}}}\bar{\boldsymbol{J}} \\ \boldsymbol{0} \end{bmatrix}, \tag{A.4}$$

$$\sqrt{\boldsymbol{A}}\boldsymbol{J}\boldsymbol{J}^T\sqrt{\boldsymbol{A}} = \begin{bmatrix} \sqrt{\bar{\boldsymbol{A}}}\bar{\boldsymbol{J}}\bar{\boldsymbol{J}}^T\sqrt{\bar{\boldsymbol{A}}} & \boldsymbol{0} \\ \boldsymbol{0} & \boldsymbol{0} \end{bmatrix}. \tag{A.5}$$

After some simple algebra, the formula for the pseudo-inverse $(\sqrt{\boldsymbol{A}}\boldsymbol{J})^{\#}$ becomes:

$$\begin{aligned}(\sqrt{\boldsymbol{A}}\boldsymbol{J})^{\#} &= \boldsymbol{J}^T\sqrt{\boldsymbol{A}}(\sqrt{\boldsymbol{A}}\boldsymbol{J}\boldsymbol{J}^T\sqrt{\boldsymbol{A}})^{\#} \\ &= \begin{bmatrix}\bar{\boldsymbol{J}}^{\#} & \boldsymbol{0}\end{bmatrix}\sqrt{\boldsymbol{A}}^{\#}\end{aligned} \tag{A.6}$$

which substituted into the control law (26) yields

$$\begin{aligned}\dot{\boldsymbol{y}} &= \begin{bmatrix}\bar{\boldsymbol{J}}^{\#} & \boldsymbol{0}\end{bmatrix}\boldsymbol{A}\dot{\bar{\boldsymbol{x}}} + (\boldsymbol{I} - \begin{bmatrix}\bar{\boldsymbol{J}}^{\#} & \boldsymbol{0}\end{bmatrix}\boldsymbol{A}\boldsymbol{J})\dot{\boldsymbol{z}} \\ &\triangleq \boldsymbol{\rho} + \boldsymbol{Q}\dot{\boldsymbol{z}}, \forall \dot{\boldsymbol{z}}.\end{aligned} \tag{A.7}$$

This could not be otherwise, as the added cost in (24) vanishes whenever $\boldsymbol{A}$ is composed only by ones and zeros, and thus the obtained solution is just the pseudo inverse of $\boldsymbol{J}$ with only the relevant rows.

The projection matrix $(\boldsymbol{I} - \begin{bmatrix}\bar{\boldsymbol{J}}^{\#} & \boldsymbol{0}\end{bmatrix}\boldsymbol{A}\boldsymbol{J})$ is still orthogonal to the active rows. Indeed,

$$\boldsymbol{J}\boldsymbol{Q} = \begin{bmatrix}(\boldsymbol{I} - \bar{\boldsymbol{J}}\bar{\boldsymbol{J}}^{\#}\bar{\boldsymbol{A}})\bar{\boldsymbol{J}} \\ (\boldsymbol{I} - \hat{\boldsymbol{J}}\bar{\boldsymbol{J}}^{\#}\bar{\boldsymbol{A}})\bar{\boldsymbol{J}}\end{bmatrix} \tag{A.8}$$

Again, it is easy to see that in $(\boldsymbol{I} - \bar{\boldsymbol{J}}\bar{\boldsymbol{J}}^{\#}\bar{\boldsymbol{A}})\bar{\boldsymbol{J}}$, for every linearly independent row where $A_{(i,i)} = 1$, then $(\boldsymbol{J}\boldsymbol{Q})_{\{i\}} = \boldsymbol{0}$ as it was claimed. For a set of linearly dependent rows, the orthogonality property holds if and only if all the corresponding $A_{(i,i)}$ are equal to one.

Enrico Simetti received the Ph.D. degree from University of Genova in 2012, and since 2014 he is an Assistant Professor at DIBRIS, University of Genova. His research interests are in the area of autonomous robotics and, in particular, on the development of control systems and coordination algorithms for robotic platforms, with special focus on marine robotics. He has a good background both in the theoretical and experimental parts of robotic research. Indeed, in the last few years, he developed strong skills in real time software development and in the development of embedded system software. In particular, he

has developed and coordinated most of the ISME software development in the successful TRIDENT FP7 project.

Giuseppe Casalino is currently full professor at DIBRIS, University of Genova. His research activities are in the field of Robotics and Automation, with special interests devoted to all the aspects involving planning, motion and interaction control problems within sensorized multirobot structures. Particular applicative interests are directed toward the fields of Underwater and Space Robotics. He is the Director of the Interuniversity Research Center on Integrated Systems for the Marine Environment (ISME). He is, and has been, the responsible scientist of many EEC funded collaborative research projects and many Italian funded research projects, all in the field of robotics and automation. He is the author of more then hundred papers on the subject, published on international journal and conferences.